Published in final edited form as:
J Electroanal Chem (Lausanne Switz). 2012 August 15; 682: 141–146. doi:10.1016/j.jelechem.2012.07.014.

Implantable Microprobe with Arrayed Microsensors for Combined Amperometric Monitoring of the Neurotransmitters, Glutamate and Dopamine

Tina T.-C. Tseng[1] and **Harold G. Monbouquette**
Department of Chemical and Biomolecular Engineering Department, University of California, Los Angeles, CA 90095, USA, Tel: (310) 825-8946, Fax: (310) 206-4107

Harold G. Monbouquette: hmonbouq@ucla.edu

Abstract

An implantable, micromachined microprobe with a microsensor array for combined monitoring of the neurotransmitters, glutamate (Glut) and dopamine (DA), by constant potential amperometry has been created and characterized. Microprobe studies *in vitro* revealed Glut and DA microsensor sensitivities of 126±5 nA·μM^{-1}·cm^{-2} and 3250±50 nA·μM^{-1}·cm^{-2}, respectively, with corresponding detection limits of 2.1±0.2 μM and 62±8 nM, both at comparable ~1 sec response times. No diffusional interaction of H_2O_2 among arrayed microelectrodes was observed. Also, no responses from the electroactive interferents, ascorbic acid (AA), uric acid (UA), DOPA (a DA catabolite) or DOPAC (a DA precursor), over their respective physiological concentration ranges, were detected. The dual sensing microbe attributes of size, detection limit, sensitivity, response time and selectivity make it attractive for combined sensing of Glut and DA *in vivo*.

Keywords

Microelectrode array; Combined glutamate and dopamine monitoring; Constant Potential Amperometry; Biosensor

1. Introduction

Studies of the interwoven roles of multiple neurotransmitters can illuminate the mechanisms behind and the progression of neurological diseases and disorders. Investigation of the interplay between the neurotransmitters, glutamate (Glut) and dopamine (DA), is of particular interest. For example, the loss of dopaminergic neurons, which dysregulates glutamatergic transmission, underlies the symptoms observed in Parkinson's disease [1]. Also, changes in relative Glut and DA transmission in the basolateral amygdala and nucleus accumbens core may be associated with the shifts in reward seeking behavior leading to addiction [2]. Therefore, implantable analytical tools for real-time, simultaneous monitoring of Glut and DA with high spatial resolution would be very useful for neuroscience research.

Correspondence to: Harold G. Monbouquette, hmonbouq@ucla.edu.

[1]Current Address: Department of Chemical Engineering, National Taiwan University of Science and Technology, Taipei 10607, Taiwan

A number of important challenges are confronted in the design of sensing probes for neurotransmitters including subsecond response time, selectivity against the array of electroactive species present in brain extracellular fluid, and micron-scale size to reduce tissue damage and provide spatial resolution. Also low detection limit and high sensitivity are required to detect neurotransmitters commonly present in the nanomolar to micromolar range. In particular, the background extracellular concentration range of Glut is ≤ 10 μM [3] to 100 μM [4] after stimulation, while that of DA is ≤ 0.1 μM to only 1 μM after stimulation [5]. These challenges in sensor design have made the innovative development of new analytical tools for monitoring neurotransmitter levels *in vivo* an area of significant research and engineering activity for several decades.

Although microdialysis has been used widely over many years for the sampling of brain extracellular fluid *in vivo* [6] and its analysis for neurotransmitters using associated analytical equipment (*e.g.*, capillary electrophoresis coupled to laser-induced fluorescence (CE-LIF) [7,8] and liquid chromatography coupled to tandem mass spectrometry (LC-MS/MS) [9,10]), the long analysis times (5–10 min) and relatively large probe sizes (≥200 μm) gives this tool inadequate temporal and spatial resolution for many studies [7–11]. Micromachined microelectrode array microprobes with customizable microelectrode design of well-defined micron-size area can provide better spatial resolution. Further, their smaller size results in infliction of less tissue damage during implantation while still providing good mechanical strength [4,12–15]. A variety of electrochemical techniques may be used for sensing at the microelectrode sites, yet constant potential amperometry offers the best temporal resolution with sampling rates down to 1 ms [16]. Although fast-scan cyclic voltammetry (FSCV) has proven to be an excellent electrochemical detection method for a number of electroactive neurotransmitters, principally DA [17,18], it requires specialized instrumentation. In contrast, constant potential amperometry requires only a standard potentiostat and straightforward collection and analysis of current signals obtained at a constant applied potential. Constant potential amperometry therefore is the preferred electroanalytical technique for monitoring neurotransmitter levels when the major electrooxidizable species are known and electroactive interferents either are selectively excluded from the sensing electrode surface or are below the detection limit [17,19].

Sensor selectivity against interferents can be achieved by modifying the electrode surfaces with suitable permselective polymers at the electrode surface. The perfluoronated ionomer, Nafion, commonly is used to exclude anionic interferents [20]. Overoxidized polypyrrole (OPPy) also has been deposited on electrodes, commonly as a permselective cation-exchange film [18,21]. OPPy films are created by first electropolymerizing pyrrole to form polypyrrole followed by its electrooxidation at high potential in the absence of monomer. The electronegative carbonyl groups formed along the OPPy backbone during electrooxidation can effectively attract cations and repel anions [22]. In fact, a thin OPPy film has been found to improve the sensitivity of electrochemical DA sensors by enhancing DA adsorption at the electrode surface [18]. However, it also has been reported that relatively thick, ~100 nm OPPy films reject both negatively charged ascorbic acid and positively charged DA, but allow the ready permeation of small neutral molecules, such as hydrogen peroxide (H_2O_2) [4,23–26], presumably because the incomplete electrooxidation of thick polypyrrole films results in a deposit of layered electropositive and electronegative character. Such thick OPPy films have proved invaluable in the construction of selective Glut sensors [4,23,25].

Most Glut sensor designs rely on the use of glutamate oxidase (GlutOx) as the selective sensing element. GlutOx catalyzes the oxidative deamination of Glut in the presence of oxygen to produce α-ketoglutarate, ammonia, and H_2O_2 [27]. The neutral and electroactive H_2O_2 species can pass through permselective polymers designed to block charged

electroactive interferents from an underlying electrode and can be electrooxidized at constant potential to give a current signal. Pt generally [24,28] is the electrode material of choice for electrooxidation of H_2O_2 rather than other common materials, such as Au, Pd, and glassy carbon (GC). Glut sensors based on cylindrical Pt microelectrodes [25,29–31] or on Pt microelectrode array microprobes, including those micromachined from silicon wafers [4] and from ceramic substrates [13,23], have shown promising results *in vivo* for the selective monitoring of Glut in near real time.

However, the sensing of the electroactive DA species has been reported to present a different set of sensor design issues, most often cited are those related to electrode fouling and selectivity. Carbon fiber (CF) microelectrodes have been shown to undergo little or no fouling by the products of DA electrooxidation, and CF electrodes combined with FSCV have been employed with notable success to monitor DA release *in vivo* [32–34]; however as mentioned above, FSCV requires specialized instrumentation and less straightforward data analysis than constant potential amperometry. The issue of electrode fouling when DA oxidation occurs at the noble metal electrode surface, such as platinum (Pt) [35] and gold [36], has been mentioned frequently, and therefore, the feasibility of using Pt electrodes for analytical determination of DA has been viewed as questionable. Some alternative DA sensor designs have been explored that are based on an electoenzymatic approach utilizing the enzymes, tyrosinase [37] and polyphenol oxidase [29]; but these enzymes are not selective for DA. Other promising DA sensors have been constructed with new materials, including graphene [38] and carbon nanotubes [39, 40], but some important sensor design issues (*e.g.,* response time, selectivity, *etc.*) must be further investigated. DA microelectrode array sensors based on FSCV [15] and constant potential amperometry [12] also have been reported recently. However, there remains a need for the development of a DA sensor with the desired attributes of detection limit, sensitivity, selectivity and response time that can readily be incorporated in a common probe with the successful Glut sensors previously developed [4] that are based on straightforward, constant potential amperometry. In this study, we describe a potentially implantable microprobe with OPPy/Nafion-modified Pt microelectrode array microsensors for combined, near-real-time monitoring of non-electroactive Glut and electroactive DA with high sensitivity and selectivity as well as adequate detection limit.

2. Experimental

2.1 Materials

Pyrrole, Nafion® (5%), glutaraldehyde solution (25%), bovine serum albumin (BSA) lyophilized powder, hydrogen peroxide solution (30%), L-glutamic acid, L-ascorbic acid, dopamine hydrochloride, 3,4-dihydroxyphenylacetic acid, 3,4-dihydroxy-DL-phenylalanine, uric acid, (−)-epinephrine (+)-bitartrate salt, DL-norepinephrine hydrochloride, and serotonin hydrochloride were purchased from Sigma-Aldrich (St. Louis, MO). Isopropyl alcohol and sulfuric acid 1 N solution were obtained from Fisher Scientific (Pittsburgh, PA). L-Glutamate oxidase (EC 1.4.3.11) from *Streptomyces* sp. X119-6, with a rated activity of 24.9 units per mg protein, produced by Yamasa Corporation (Chiba, Japan), was obtained from Associates of Cape Cod, Inc. (Northstar BioProducts®, East Falmouth, MA). Silicon wafers (diameter: 4 inch; p-type boron doped; orientation <1 0 0>; thickness: 150 ± 15 μm) were purchased from Silicon Valley Microelectronics (Santa Clara, CA). Ag/AgCl glass-bodied reference electrodes with 3 M NaCl electrolyte and a 0.5 mm diameter platinum (Pt) wire auxiliary electrode were purchased from BASi (West Lafayette, IN). Sodium phosphate buffer (PBS) was composed of 50 mM sodium phosphate (dibasic) and 100 mM sodium chloride (pH 7.4).

2.2 Instrumentation

Electrochemical experiments for sensor development and initial evaluation were performed using a Versatile Multichannel Potentiostat (model VMP3) equipped with the 'p' low current option and N'Stat box driven by EC-LAB software (Bio-Logic USA, LLC, Knoxville, TN) in a three-electrode configuration consisting of the sensing electrode, a Pt wire auxiliary electrode, and a Ag/AgCl glass-bodied reference electrode. Sensor calibration was conducted on a multichannel FAST-16 potentiostat (Quanteon, LLC, Lexington, KY) in two-electrode mode with a glass-bodied Ag/AgCl reference electrode.

2.3 Microprobe fabrication and sensor preparation

First, a 1 μm layer of silicon dioxide on a 4-inch silicon wafer (150 ± 15 μm in thickness) was grown by thermal oxidation. After a photolithographic patterning step, a Pt layer was deposited using an electron-beam evaporator to define bonding pads, microelectrode sites, and channel leads. Insulating layers were deposited using plasma enhanced chemical vapor deposition. After a second photolithography step, the insulating layers were dry etched to create openings at the bonding pads and electrode sites. Finally to make each probe releasable, the silicon substrate was etched through using reactive ion etching after a third photolithography step (see Figure 1 for a microprobe fabrication overview). A 2×2 microelectrode array was located at the tip (120 μm in width and 150 μm in thickness) of the microprobe with 100 μm vertical and 40 μm lateral separations between the microelectrodes. Each microelectrode had an average area of ~5000 μm^2.

Microelectrodes were rinsed with isopropyl alcohol followed by an electrochemical cleaning step with 1 N sulfuric acid before administering modifications tailored to analyte sensing. Selective electrodeposition of thin PPy films (2 mM Py in PBS, 20 mV/sec, 0.2 V to 1.2 V, 2 cycles) was carried out at bottom sites for DA sensing, while thick PPy films were electrodeposited (200 mM Py in stirred PBS, 0.85 V, ~5 min) at top sites for Glut sensing. Electrodeposition was followed by PPy over-oxidation at 989 mV (*vs.* Ag/AgCl) for ≥40 min (until a stable current response was reached). Microelectrodes were dip-coated with 1% Nafion solution and then baked for 3 min at 180 °C (repeated 8 times). GlutOx was selectively immobilized on the top left electrode site (Figure 2a) using a microsyringe under the microscope. The GlutOx solution for enzyme immobilization was prepared by mixing 2 μL GlutOx (250 unit/mL) with 3 μL BSA solution (10 mg/mL) containing glutaraldehyde (0.125 % v/v). The resulting dual Glut/DA sensor microprobe was left to dry overnight in a dessicator at 4°C. The final sensor configuration is shown in Figure 2b. Before making measurements, ≥30 min of equilibrium time in sodium phosphate buffer (PBS) was required for the current detected from the dual sensor to approach a constant baseline.

3. Results and discussion

3.1 Evaluation of DA fouling on Pt microelectrodes

Bare Pt microelectrode fouling was evaluated over a range of DA concentrations by cyclic voltammetry. Although several prior studies [35,36] indicated that the DA electrooxidation product can polymerize and form an insulating film on noble metal electrode surfaces, we found that fouling occurs only at excessively high DA concentrations. As shown in Figure 3, repeated potential cycling at bare Pt microelectrodes gave stable voltammograms in DA solutions up to at least 800 μM, which is far beyond the physiological concentration of DA in the central nervous system [5]. At 4 mM DA, the previously reported fouling was observed, as evidenced by the decrease in DA oxidation peak amplitude with each successive cycle. These results provided a promising basis for construction of a useful Pt microelectrode sensor for DA in the physiological concentration range.

3.2 DA sensor and combined sensing of Glut and DA

The microprobe constructed with DA sensors (Pt microelectrodes modified with thin OPPy and Nafion) and control sensors (Pt microelectrodes modified with thick OPPy and Nafion) was first tested *in vitro* at 0.7 V (*vs.* Ag/Ag/Cl) in stirred PBS. As shown in Figure 4, for DA sensors, no detectable response was observed in the presence of the negatively charged electroactive interferent, ascorbic acid (AA), at up to 750 μM; in addition, the DA sensors showed highly sensitive responses with fast temporal resolution (~1 sec) upon DA injections. These promising results suggested that the optimized combination of electronegative, thin OPPy and negatively charged Nafion not only can repel AA at physiological concentrations (usually ranging from 10–200 μM) [41,42], but also can preconcentrate cationic DA at the electrode surface without sacrificing the DA sensing response time. On the other hand, at control microelectrode sites, no response was observed in the presence of either DA or AA suggesting that the combination of thick OPPy and negatively charged Nafion can reject effectively these charged species. This result is consistent with earlier reports that relatively thick OPPy can reject both positively charged DA and negatively charged AA [4,23–26]. Both DA sensing sites and control sites responded to H_2O_2 indicating that the small, neutral H_2O_2 molecule can pass through both permselective polymer layer combinations and react at the Pt electrode surface at 0.7 V with good sensitivity and response time.

The dual mode Glut/DA sensor was constructed by further modifying one of the control sites described above with the GlutOx immobilization matrix. The resulting dual Glut/DA sensor was tested *in vitro* at +0.7 V (*vs.* Ag/AgCl) in stirred PBS. Again, in the presence of AA at 250 μM no response was observed from all sensor sites (Figure 5). Upon the addition of Glut, only the Glut sensor site (modified with thick OPPy, Nafion, and GlutOx) responded to Glut injections with ~1 sec response time as indicated by the step signal shown; while in the presence of DA, only the DA sensor site (modified with thin OPPy and Nafion) responded to DA additions. The control site (modified with thick OPPy and Nafion; without GlutOx) did not give any detectable responses to AA, Glut, and DA, only to H_2O_2. In summary: (1) the thick OPPy and Nafion modified permselective films discriminated the small neutral H_2O_2 molecule from anionic and cationic electroactive species (*i.e.*, AA and DA, respectively) [4,23–26] as desired, (2) the detected responses from the Glut sensor site upon Glut additions were from GlutOx-catalyzed generation of H_2O_2, (3) the thin OPPy and Nafion modified permselective films on the DA sensor site excluded negatively charged AA, but permited access of positively charged DA [18,21], and (4) no diffusional interaction (or crosstalk) of H_2O_2 generated from the Glut sensor site to other closely arrayed microsensors (≥40 μm separation) on the same probe occurred [43]. This dual Glut/DA sensing data suggests the feasibility of combined monitoring of Glut and DA, provided the required sensitivity and detection limit as well as selectivity against other electroactive species can be attained.

3.3 Dual Glut/DA sensor calibration curves

Typical calibration curves for the dual Glut/DA sensor are presented in Figure 6. Based on the calibration curve slope in the linear range, the Glut microsensor exhibited a sensitivity of 126±5 $nA \cdot \mu M^{-1} \cdot cm^{-2}$ and the DA microsensor had a sensitivity 3250±50 $nA \cdot \mu M^{-1} \cdot cm^{-2}$ (n = 3). The detection limits at two times the level of noise were 2.1±0.2 μM for Glut and 62±8 nM for DA (n = 3). The dual sensor displayed a detection range of up to ≥630 μM for Glut and up to ≥40 μM for DA, which is suitable for sensing physiological concentrations of both DA and Glut [3,5]. Although the DA detection limit is somewhat higher than that reported for FSCV (~25 nM), it still is sufficient to record the naturally occurring transients in DA concentration of 0.1 – >1 μM observed in freely moving rats, for example [17]. Thus, the response time, sensitivity and detection limit of the combined microsensor were suggestive

of its utility for study of the interplay of Glut and DA transmission *in vivo*, provided sensor selectivity against a broader array of electroactive interferents could be demonstrated.

3.4 Selectivity against electroactive interferents

The selectivity against interferents was evaluated for both the Glut and DA microsensors (with selectivity defined here as the ratio of sensitivity to the analyte divided by that for the interferent). The Glut microsensor showed excellent selectivity for Glut against the interferents tested, including AA, DA, DOPAC, DOPA, epinephrine (EP), norepinephrine (NEP), uric acid (UA), and serotonin; whereas the DA microsensor showed excellent selectivity for DA against AA, DOPAC, DOPA, and UA at (or more than) typical physiological concentrations. Average selectivity ratios of Glut to AA (250 μM), DA (12.5 μM), DOPAC (50 μM), DOPA (50 μM), EP (12.5 μM), NEP (12.5 μM), UA (250 μM), and serotonin (5 μM) were all more than at least 1000 : 1 for the Glut microsensor (where the maximum tested concentration of the interferent is given in parentheses); and average selectivity ratios of DA to AA (250 μM), DOPAC (50 μM), DOPA (50 μM), and UA (250 μM) were all more than at least 1000 : 1 for the DA microsensor as well. However, the DA microsensor selectivity for DA over EP and NEP was only ~1.2 and ~2.3, respectively, due to their similar chemical structures and oxidation potentials. Fortunately, the basal levels of EP (≤5 nM) [44], NEP (1–50 nM) [45,46], and serotonin (~2 nM) [47–51] all are below the detection limits of our DA sensor for these species (~200 nM, ~230 nM, ~290 nM, respectively). As a point of comparison, the popular FSCV method also does not enable differentiation of EP and NEP from DA [18]. Thus, the application of our proposed DA sensor *in vivo* is valid in general when DA is known as the major oxidizable compound around the electrode and interferents are excluded from the electrode surface or are below the detection limit.

4. Conclusion

In summary, a convenient implantable microprobe with microelectrode array sensors has been created and characterized for near-real-time combined sensing of the non-electroactive and electroactive neurotransmitters, glutamate and dopamine, respectively, at microelectrodes in close proximity to one another (~40 μm) on the same microprobe. Building upon previous breakthroughs in selective, near real time glutamate sensing [4], the highly sensitive and selective dual mode Glut/DA sensor provides high spatial resolution, fast response time, and suitable detection ranges for both analytes without any detectable H_2O_2-mediated crosstalk between Glut and DA microelectrode sites. Future applications of the described dual mode sensor in laboratory rodents may shed light on the role of glutamate and dopamine transmission in mechanisms underlying important fundamental behaviors as well as neurological diseases and disorders.

Acknowledgments

This research was supported by a NIH grant (R21NS064547) to HM. The authors thank Dr. Vanessa Tolosa and Dr. Kate Wassum for their valuable suggestions on sensor design and preparation, and Dr. Nigel Maidment for generously providing the potentiostat for *in vitro* sensor calibration.

References

1. Lange KW, Kornhuber J, Riederer P. Neurosci Biobehav Rev. 1997; 21:393–400. [PubMed: 9195597]
2. Everitt BJ, Robbins TW. Nat Neurosci. 2005; 8:1481–1489. [PubMed: 16251991]
3. Espey MG, Kustova Y, Sei Y, Basile AS. J Neurochem. 1998; 71:2079–2087. [PubMed: 9798933]

4. Wassum KM, Tolosa VM, Wang J, Walker E, Monbouquette HG, Maidment NT. Sensors. 2008; 8:5023–5036. [PubMed: 19543440]
5. Iniouchine MY, Sibarov DA, Volnova AB, Jimenez-Rivera CA, Nozdrachev AD. Dokl Biol Sci. 2008; 419:80–82. [PubMed: 18536267]
6. Chefer VI, Thompson AC, Zapata A, Shippenberg TS. Curr Protoc Neurosci. Apr.2009 :7.1.1–7.1.28.
7. Zhang D, Zhang J, Ma W, Chen D, Han H, Shu H, Liu G. J Chromatogr B. 2001; 758:277–282.
8. Bowser MT, Kennedy RT. Electrophoresis. 2001; 22:3668–3676. [PubMed: 11699904]
9. Uutela P, Ketola RA, Piepponen P, Kostiainen R. Anal Chim Acta. 2009; 633:223–231. [PubMed: 19166726]
10. Hows MEP, Lacroix L, Heidbreder C, Organ AJ, Shah AJ. J Neurosci Meth. 2004; 138:123–132.
11. Zhang MY, Beyer CE. J Pharm Biomed Anal. 2006; 40:492–499. [PubMed: 16125893]
12. Johnson MD, Franklin RK, Gibson MD, Brown RB, Kipke DR. J Neurosci Meth. 2008; 174:62–70.
13. Burmeister JJ, Pomerleau F, Palmer M, Day BK, Huettl P, Gerhardt GA. J Neurosci Methods. 2002; 119:163–171. [PubMed: 12323420]
14. Wise KD, Sodagar AM, Yao Y, Gulari MN, Perlin GE, Najafi K. Proc IEEE. 2008; 96:1184–1202.
15. Zachek MK, Park J, Takmakov P, Wightman RM, McCarty GS. Analyst. 2010; 135:1556–1563. [PubMed: 20464031]
16. Dugast C, Suaud-Chagny MF, Gonon F. Neurosci. 1994; 62:647–654.
17. Robinson DL, Venton BJ, Heien MLAV, Wightman RM. Clin Chem. 2003; 49:1763–1773. [PubMed: 14500617]
18. Pihel K, Walker QD, Wightman RM. Anal Chem. 1996; 68:2084–2089. [PubMed: 9027223]
19. Benoit-Marand, M.; Suaud-Chagny, M.; Gonon, F. Electrochemical Methods for Neuroscience. Michael, AC.; Borland, LM., editors. CRC Press; Boca Raton: 2007. p. 35-47.
20. Gerhardt GA, Oke AF, Nagy G, Moghaddam B, Adams RN. Brain Res. 1984; 290:390–395. [PubMed: 6692152]
21. Hsueh C, Brajter-Toth A. Anal Chem. 1994; 66:2458–2464.
22. Beck F, Braun P, Oberst M. Ber Bunsen-Ges Phys Chem. 1987; 91:967–974.
23. Walker E, Wang J, Hamdi N, Monbouquette HG, Maidment NT. Analyst. 2007; 132:1107–1111. [PubMed: 17955144]
24. Hamdi N, Wang J, Monbouquette HG. J Electroanal Chem. 2005; 581:258–264.
25. Hamdi N, Wang J, Walker E, Maidment NT, Monbouquette HG. J Electroanal Chem. 2006; 591:33–40.
26. Debiemme-Chouvy C. Biosens Bioelectron. 2010; 25:2454–2457. [PubMed: 20434323]
27. Kusakabe H, Midorikawa Y, Fujishima T, Kuninaka A, Yoshino H. Agric Biol Chem. 1983; 47:1323–1328.
28. O'Neill RD, Chang S-C, Lowry JP, McNeil CJ. Biosens Bioelectron. 2004; 19:1521–1528. [PubMed: 15093225]
29. Cosnier S, Innocent C, Allien L, Poitry S, Tsacopoulos M. Anal Chem. 1997; 69:968–971. [PubMed: 21639234]
30. Lowry JP, Ryan MR, O'Neill RD. Anal Commun. 1998; 35:87–89.
31. Cooper JM, Foreman PL, Glidle A, Ling TW, Pritchard DJ. J Electroanal Chem. 1995; 388:143–149.
32. Rebec GV, Christensen JRC, Guerra C, Bardo MT. Brain Res. 1997; 776:61–67. [PubMed: 9439796]
33. Stamford JA, Kruk ZL, Millar J, Wightman RM. Neurosci Lett. 1984; 51:133–138. [PubMed: 6334821]
34. Heien MLAV, Khan AS, Ariansen JL, Cheer JF, Phillips PEM, Wassum KM, Wightman RM. Proc Nat Acad Sci USA. 2005; 102:10023–10028. [PubMed: 16006505]
35. Lane RF, Hubbard AT. Anal Chem. 1976; 48:1287–1293. [PubMed: 952392]
36. Łuczac T. Electrochim Acta. 2008; 53:5725–5731.

37. Njagi J, Chernov MM, Leiter JC, Andreescu S. Anal Chem. 2010; 82:989–996. [PubMed: 20055419]
38. Wang Y, Li Y, Tang L, Lu J, Li J. Electrochem Commun. 2009; 11:889–892.
39. Swamy BEK, Venton BJ. Analyst. 2007; 132:876–884. [PubMed: 17710262]
40. Hočevar SB, Wang J, Deo RP, Musameh M, Ogorevc B. Electroanal. 2005; 17:417–422.
41. Hallström A, Carlsson Å, Hillered L, Ungerstedt U. J Pharm Meth. 1989; 21:113–124.
42. Spector R. New Eng J Med. 1977; 296:1393–1398. [PubMed: 323714]
43. Baur JE, Miller HM, Ritchason MA. Anal Chim Acta. 1999; 397:123–133.
44. Dev BR, Mason PA, Freed CR. J Neurochem. 1992; 58:1386–1394. [PubMed: 1372344]
45. Zini R, Tillement JP, Morin D. Biologie & Santé. 2000; 1:6–13.
46. Devoto P, Flore G, Pani L, Gessa GL. Mol Psychiatry. 2001; 6:657–664. [PubMed: 11673793]
47. Béquet F, Gomez-Merino D, Berthelot M, Guezennec CY. Acta Physiol Scand. 2001; 173:223–230. [PubMed: 11683680]
48. Wright IK, Upton N, Marsden CA. Psychopharmacology. 1992; 109:338–346. [PubMed: 1285416]
49. Parsons LH, Koob GF, Weiss F. Behav Brain Res. 1996; 73:225–228. [PubMed: 8788507]
50. Kalén P, Strecker RE, Rosengren E, Björklund A. J Neurochem. 1988; 51:1422–1435. [PubMed: 2459309]
51. Invernizzi R, Belli S, Samanin R. Brain Res. 1992; 584:322–324. [PubMed: 1515949]

Highlights

- Near-real-time combined sensing of the neurotransmitters, glutamate and dopamine
- Good selectivity, fast response time, and suitable detection ranges for both analytes
- No detectable H_2O_2-mediated crosstalk between Glut and DA microelectrode sites
- Probe useful for studying the role of Glut and DA in neurological diseases

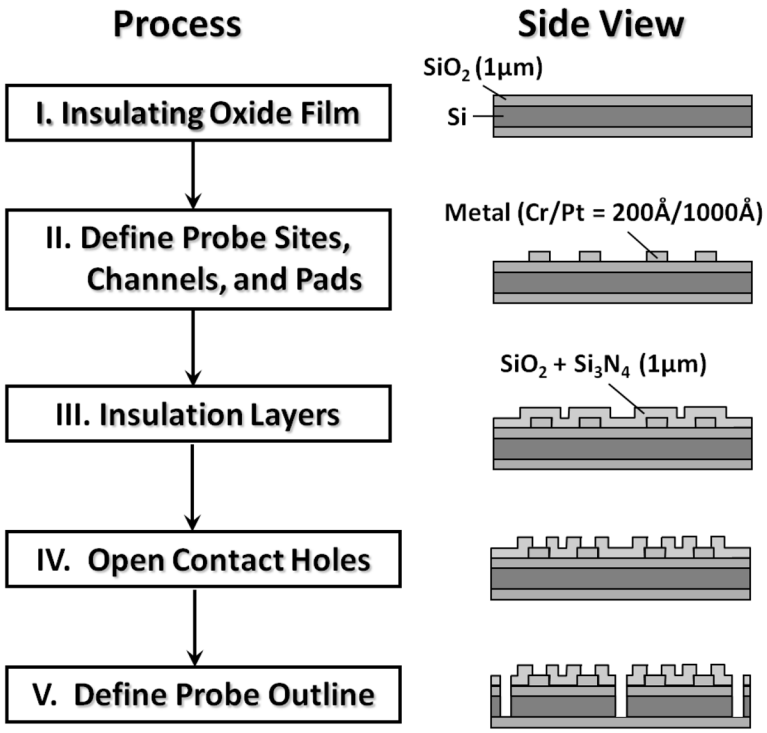

Figure 1.
Micromachined microprobe fabrication overview.

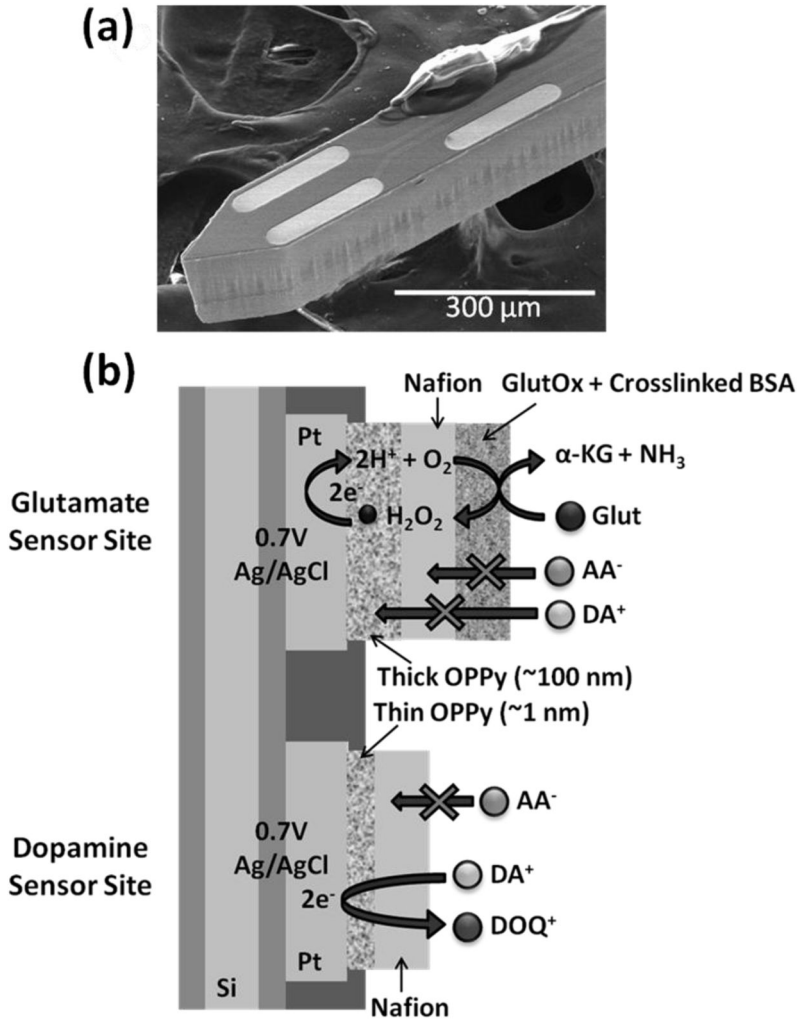

Figure 2.

(a) Scanning electron microscopy (SEM) image of selective GlutOx immobilization on the top left microelectrode site previously modified with a thick OPPy film and Nafion. (b) Schematic diagram of the final dual Glut/DA sensor configuration.

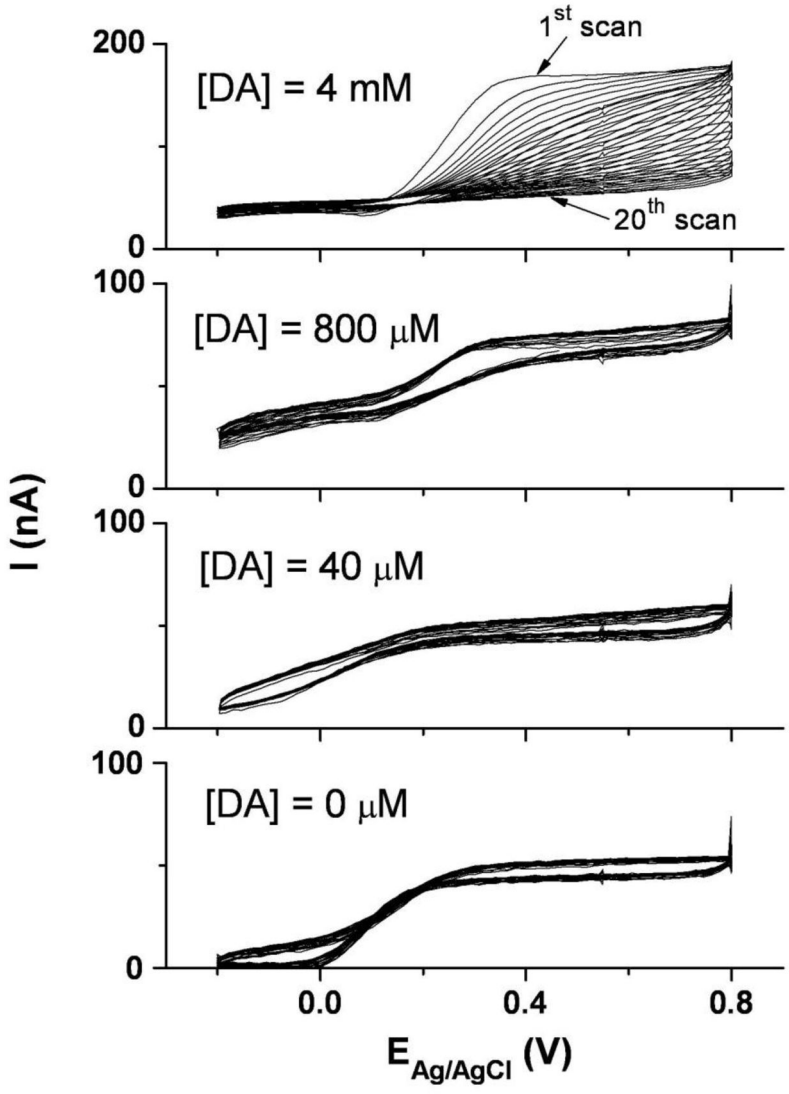

Figure 3.
Repeated cyclic voltammograms with bare Pt microelectrodes in dopamine solutions of varied concentration (0 μM, 40 μM, 800 μM, and 4 mM in 50 mM PBS, pH 7.4). The scan rate was 100 mV/sec conducted over the range, −0.2 V to 0.8 V, for 20 cycles.

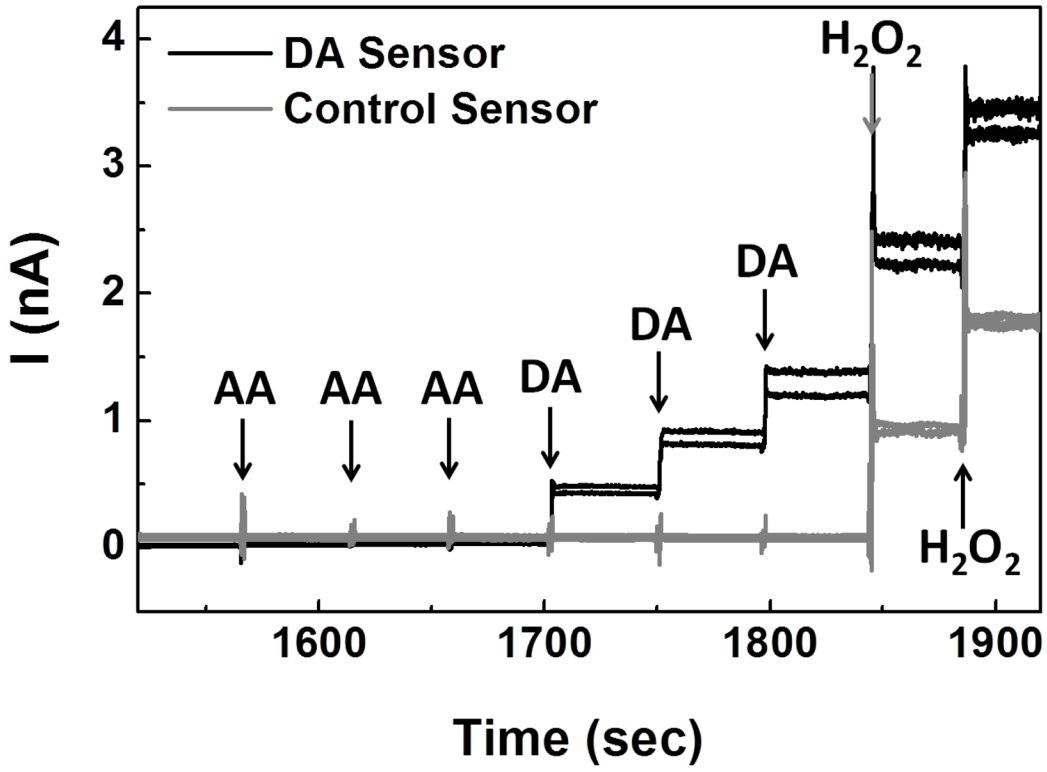

Figure 4.
Microprobe with two DA sensing sites and two control sites was tested with steps in concentration of AA (250 μM, 500 μM, 750 μM), DA (5 μM, 10 μM), and H_2O_2 (10 μM, 20 μM) in 50 mM PBS, pH 7.4, at 0.7 V (*vs.* Ag/AgCl).

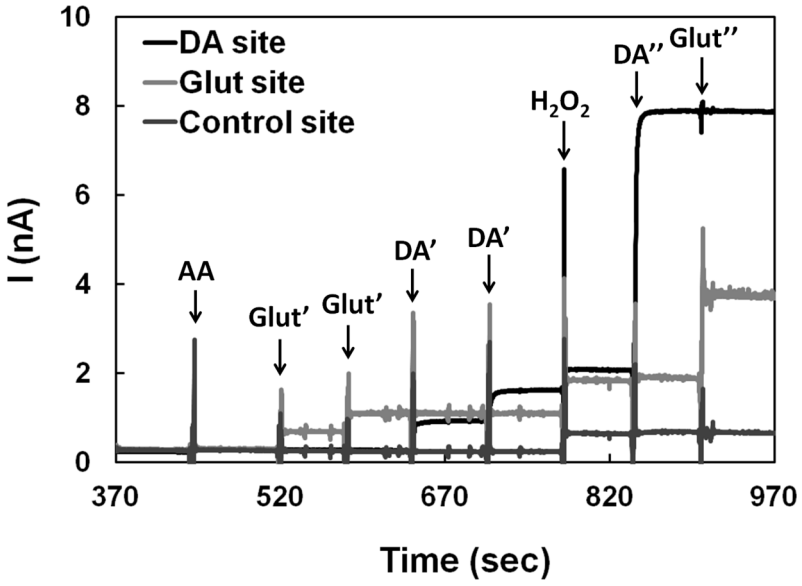

Figure 5.

Combined sensing of Glut and DA at a constant potential of 0.7 V (*vs.* Ag/AgCl). The microprobe was tested with AA (250 μM), Glut (20 μM, 40 μM), DA (5 μM, 10 μM), H_2O_2 (10 μM), DA (60 μM), and Glut (140 μM), sequentially. The first two injections resulting in Glut concentrations of 20 μM and 40 μM are denoted as Glut′ and the latter injection at higher Glut concentration giving 140 μM is denoted as Glut″. Similarly, the first two injections resulting in DA concentrations of 5 μM and 10 μM are denoted as DA′ and the latter injection at higher DA concentration giving 60 μM is denoted as DA″.

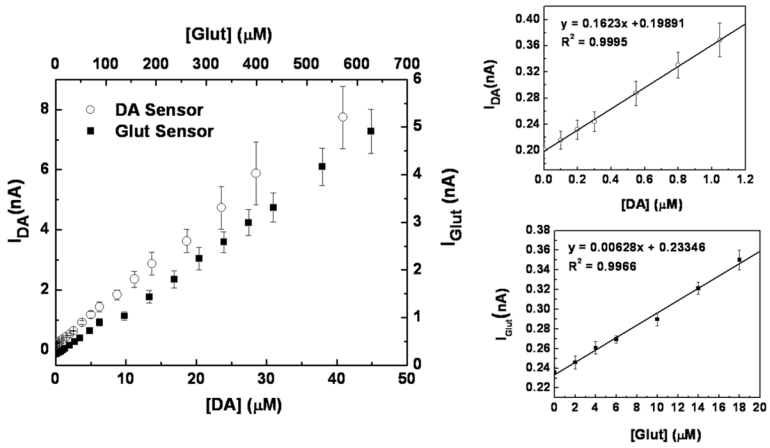

Figure 6.

Dual mode Glut/DA sensor calibration curves for Glut and DA. The smaller plots show the lower concentration ranges for each analyte. The calibrations were performed by successive injections of known Glut or DA solutions into the well-stirred cell with sensors at a constant potential of 0.7 V (*vs.* Ag/AgCl) in 50 mM PBS, pH 7.4.